JOURNAL OF MATERIALS SCIENCE LETTERS 13 (1994) 802–805

Weld metal/ferritic steel interface in laser welded austenitic/ferritic dissimilar steel joints

ZHENG SUN
Laboratory of Production Engineering, VTT, Box 111, 02151, Espoo, Finland

TAPANI MOISIO
Lappeenranta University of Technology, Box 20, 53851, Lappeenranta, Finland

Austenitic/ferritic dissimilar steel joints are widely used in power generation systems. Such joints are normally produced using conventional welding processes such as tungsten inert gas welding and manual arc welding. Research and application experiences have proved that nickel based filler is preferable for producing an austenitic/ferritic joint when using conventional welding processes [1–5]. Laser beam welding has, in recent years, attracted more attention due to its special features: a small heat-affected zone (HAZ) and narrow weld bead due to the low heat input; welding at high speed; welding can be carried out in areas of difficult access; contactless energy transfer; welding in an exact and reproducible manner; possibilities for automation and robotization, and welding performed in various atmospheres [6]. Industrial application potentials of laser welding are being actively investigated worldwide. Laser welding of dissimilar metals has also been a topic of interest recently. The possibility of using a laser to weld austenitic/ferritic dissimilar metal joints and the effects of processing parameters have been reported [7, 8]. Weld metal/ferritic steel interfacial microstructure and properties have been a critical issue for austenitic/ferritic dissimilar steel joints. Since it is the weak point of the joints, considerable efforts have been devoted to characterize it and to understand its influence on the quality of the joints made by conventional welding processes [9–13]. Data for such interfaces of laser welding joints is, however, limited, but still very important. In the present study, a high power CO_2 laser was used to join an austenitic stainless steel to a low alloy ferritic steel. The joints were produced in two modes: autogenous welding (without filler) and welding with nickel based filler wire. The interfacial microstructure between the weld metal and ferritic steel was examined in both the as-welded and post-weld heat treated conditions. The objective of this letter is to report some results concerning the interface made by laser welding in order to provide useful knowledge for assessing the process.

Base materials were AISI 347 austenitic and 13CrMo44 low alloy steel tubes with 43.5 mm outside diameter, 4.5 mm wall thickness and length of 23 mm. The chemical compositions of the base materials are listed in Table I. The filler wire used in the present study was commercial nickel based ENiCrMo-3 of diameter 1.2 mm.

Laser welding was performed using a continuous wave CO_2 laser. Plasma control and shielding gases (helium) at flow rates of 20 and 32 l min^{-1}, respectively, were used. The welding nozzle, wire feed and workpiece arrangement is shown schematically in Fig. 1. Welding parameters are given in Table II. The tube/tube joints were cut after welding, and some of them were heat treated at 650 °C for 1 h. The metallographic samples were prepared using standard procedures including grinding, polishing and etching. Optical and electron microscopy were used, with energy dispersive X-ray spectroscopy (EDS) and electron probe microanalysis (EPMA) for analysing major alloying elements.

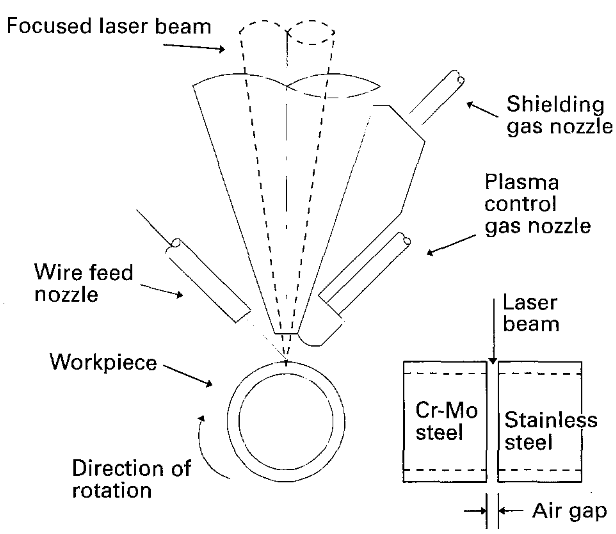

Figure 1 Schematic diagram of experimental apparatus showing laser welding nozzle, wire feed and workpiece arrangement.

TABLE I Chemical compositions of the base metals (wt %)

	C	Si	Mn	P	S	Cr	Ni	Nb	Mo	Fe
AISI 347	0.042	0.50	1.56	0.024	0.005	17.9	9.3	0.67	–	Balance
13CrMo44	0.17	0.20	0.60	0.013	0.002	0.87	–	–	0.47	Balance

TABLE II Laser welding parameters

Weld	Power (kW)	Speed (mm min^{-1})	Air gap (mm)	Wire feed rate (mm/min^{-1})
1	3.5	1250	0	0
2	3.0	900	0	0
3	3.5	1250	0.2	1125

The weld metal/ferritic steel interface was observed using an optical microscope. In the as-welded condition, there is a light etching band along the fusion line between the weld metal and ferritic steel. However, a dark etching band along the interface between the weld metal and the ferritic steel HAZ was observed in all specimens that had been heat treated after welding. The width of this dark etching band varied along the fusion line of each weld. Nonetheless, the width of the dark etching band is in the range of 10–50 μm depending on the processing conditions. In general, the dark etching zone is much larger in autogenous welds than in filler wire welds (around twice as large). Hardness tests showed the dark etching zone to be harder than both the ferritic base metal and the weld metal (see Fig. 2). Similar dark etching zones have been observed in the conventional welded austenitic/ferritic joints [9–13].

EDS analysis was made on the dark etching zone. Several positions were analysed, indicated by the numbers in Fig. 3a, with values shown in Table III. The measuring area for each point was about 20 μm^2. Because the carbon levels could not be obtained from the EDS analysis, an average carbon content for the two base metals (0.106 wt %) was used when calculating the chromium and nickel equivalents in order to plot the results on a Schaeffler diagram (Fig. 3b). The dark etching zone can be seen to be in the martensite region of the diagram. Although a discrepancy in the assumed carbon content may lead to errors in calculating the nickel equivalents, its influence will only result in changes in the vertical direction when plotting on the Schaeffler diagram. It is estimated that the maximum variation in the Ni equivalent is around 2 wt %. This is not sufficient to move the locations of the measured points outside the martensite region.

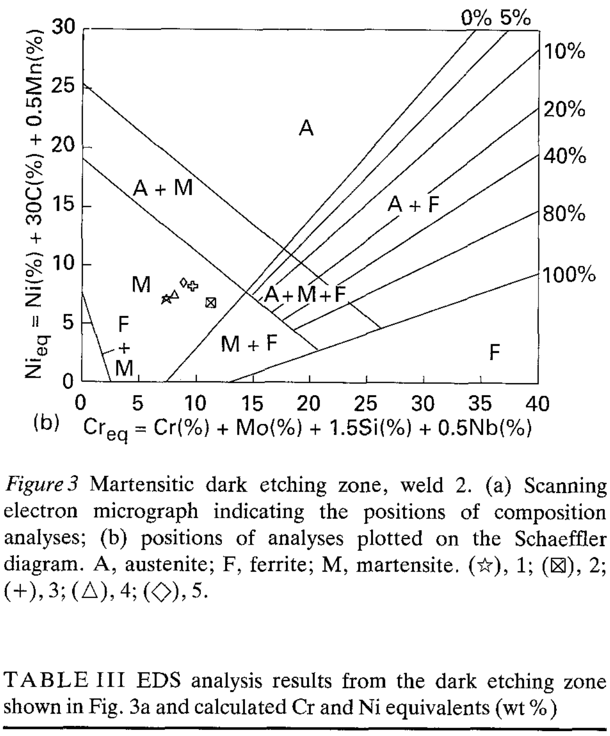

Figure 3 Martensitic dark etching zone, weld 2. (a) Scanning electron micrograph indicating the positions of composition analyses; (b) positions of analyses plotted on the Schaeffler diagram. A, austenite; F, ferrite; M, martensite. (☆), 1; (⊠), 2; (+), 3; (△), 4; (◇), 5.

TABLE III EDS analysis results from the dark etching zone shown in Fig. 3a and calculated Cr and Ni equivalents (wt %)

Position	Cr	Ni	Mn	Mo	Nb	Si	Cr_{eq}	Ni_{eq}
1	6.9	3.4	1.0	0	0	0.3	7.4	7.1
2	6.3	3.2	0.9	3.3	2.3	0.3	11.3	6.8
3	8.7	4.4	1.2	0	1.0	0.3	9.7	8.2
4	7.5	3.8	1.0	0	0	0.4	8.1	7.5
5	8.3	4.7	1.2	0	0	0.4	8.9	8.5

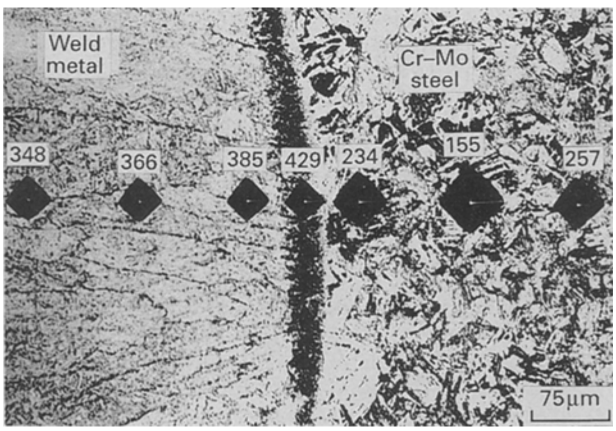

Figure 2 Optical micrograph showing the dark etching zone after PWHT of autogenous laser weld (weld 2). The numbers represent hardness in HV0.3.

EPMA measurements were also made on welds made using both autogenous welding and welding with filler wire. Fig. 4 illustrates the variation in chromium and nickel content across the interface between the weld metal and ferritic steel. It can be seen that the interface between the weld metal and ferritic steel extended a distance of about 50 μm. The composition in this region is predicted to give martensite according to the Schaeffler diagram.

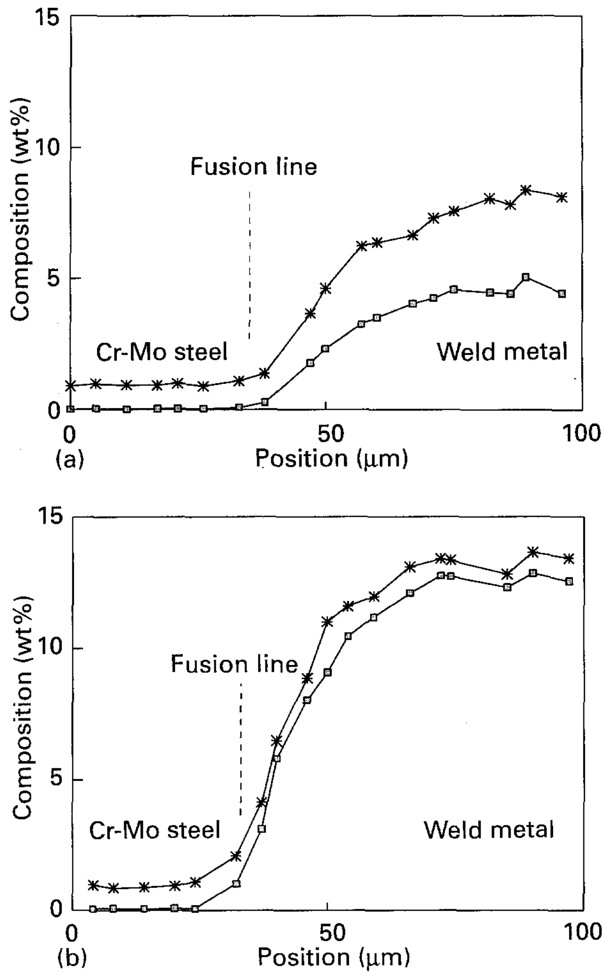

Figure 4 EPMA results showing (□) nickel and (∗) chromium profiles across the fusion line region between ferritic steel and weld metal: (a) weld 1, (b) weld 3.

It can be deduced from the above results that the dark etching zone contains martensite. It has been suggested that, in the as-welded condition, the light etching phase is martensite resulting from dilution of the weld metal by ferritic steel. After post-weld heat treatment (PWHT) tempering of the martensite produced the dark etching phase [9, 12]. It has also been argued that the filler metal (high in Ni and Cr) mixed with the ferritic parent metal (high in carbon) can produce a hardenable steel of unknown composition at the fusion line of dissimilar metal welds [14]. This composition, when cooled rapidly, would form martensite. In fact, the combination of materials and the rapid cooling rate of autogenous laser welding has already produced mixed microstructures of austenite and martensite in the weld metal, and martensite in the coarse-grained HAZ in ferritic steel [15]. Thus, the formation of dark etching martensite is reasonable. The explanation proposed by Wood [10] can be applied in the case of filler wire welds, which form a fully austenitic weld metal. EDS analysis in this study confirmed the composition and consequently the structure of this region to be martensite. One of the reasons why the width of this dark etching zone in autogenous welds is much larger than in filler wire welds can be explained by the composition of the regions, because the composition profiles in Fig. 4 show that the chromium and nickel contents of the transition zones in autogenous weld are much lower than those in filler wire weld, therefore a thinner martensite zone is formed in filler wire welds. Although this dark etching phase is harder than the surrounding regions, early studies indicated that it does not appear to have a very deleterious effect on the properties of the interface [11, 12]. Recent study of the interface between cladding of stainless steel of nickel alloy and the low alloy steel indicates that although the hard zone was of high tensile strength but limited tensile ductility, no tendency of unstable failure in the hard zone was observed in the fracture toughness tests at room temperature [16]. However, minimization of this hard zone would be beneficial because the hard zone will be sensitive to, e.g. hydrogen embrittlement, and may lead to failure at certain service conditions.

In summary, a narrow zone was observed at the interface, where the hardness was significantly higher than that in either the weld metal or ferritic base metal. The size of the zones varied with different processing conditions. The hard zone in autogenous welds was larger than that in welds made with nickel based filler wire. This effect can be attributed to the different compositional gradients at the interfaces caused by the filler wire material and dilution. The analysis results suggest that the hard zone at the interface contains martensite structure. Since the hard zone martensite exhibits usually high strength, but low ductility, it is beneficial to minimize such a zone. In this aspect, laser welding with nickel based filler wire demonstrates advantages over autogenous welding for such joints.

Acknowledgements

Financial support from the Finnish Ministry of Trade and Industry and Ahlstrom Machinery Oy is gratefully acknowledged.

References

1. J. F. KING, M. D. SULLIVAN and G. M. SLAUGHTER, *Welding J.* **56** (1977) 354s.
2. R. L. KLUEH and J. F. KING, *ibid.* **59** (1980) 114s.
3. C. D. LUNDIN, *ibid.* **61** (1982) 58s.
4. R. H. RYDER, D. I. ROBERTS, R. VISWANATHAN and M. PRAGER, in Proceedings of the International Conference on Trends in Welding Research, Gatlinburg, Tennessee, 18–22 May 1986, edited by S. A. David (American Society for Metals International, Metals Park, Ohio, 1986) p. 509.
5. R. D. NICHOLSON and A. T. PRICE, in "Welding dissimilar metals" (The Welding Institute, Cambridge, 1986) p. 53.
6. "Metals handbook", 9th Edn, Vol. 6 (American Society for Metals International, Metals Park, Ohio, 1983) p. 647.
7. Z. SUN and T. MOISIO, in Proceedings of the 3rd Conference on Laser Materials Processing in the Nordic Countries, 21–22 August 1991, Lappeenranta University of Technology, Finland, edited by T. Moisio, p. 123.
8. *Idem*, *Mat. Sci. Technol.* **9**(7) (1993) 603.
9. N. F. EATON and B. A. GLOSSOP, *Met. Construction Brit. Welding J.* **1** (1969) 6.
10. D. WOOD, *ibid.* **1** (1969) 134.

11. J. BARFORD, *ibid.* **1** (1969) 136.
12. W. K. C. JONES, *Welding J.* **53** (1974) 225s.
13. K. G. K. MURTI and S. SUNDARESAN, *ibid.* **64** (1985) 327s.
14. G. M. CAMPBELL, J. W. ELMER, W. S. GIBBS, D. K. MATLOCK and D. L. OLSON, in Proceedings of the Conference on Trends in Welding Research in the US, edited by S. A. David (American Society for Metals, Metals Park, Ohio) p. 442.
15. Z. SUN, Doctoral thesis, Lappeenranta University of Technology, Lappeenranta, Finland (1992).
16. M. F. GITTOS and T. G. GOOCH, *Welding J.* **71** (1992) 461s.

Received 19 October
and accepted 10 November 1993